Molecular Dynamics Characterization of the C2 Domain of Protein Kinase C β

Lucia Banci[†]*, Gabriele Cavallaro[†], Viktoria Kheifets[¶] and Daria Mochly-Rosen[¶]

[†]Centro di Risonanze Magnetiche (CERM), University of Florence, 50019 Sesto Fiorentino, Florence, Italy, and [¶]Department of Molecular Pharmacology, Stanford University School of Medicine, Stanford, CA 94305

*Address correspondence to:

Prof. Lucia Banci

Centro di Risonanze Magnetiche

University of Florence

Via Luigi Sacconi 6

50019 Sesto Fiorentino (Florence)

Italy

phone +39 055 4574263

fax +39 055 4574253

e-mail: banci@cerm.unifi.it

Running title: MD simulations of the C2 domain of βPKC

1

Abstract

Protein kinase C (PKC)[1] isozymes comprise a family of related enzymes that play a central role in many intracellular eukaryotic signaling events. Members of the PKC family are activated by lipid-derived second messengers and, upon activation, translocate from one cell compartment to another. Specificity is mediated by association of each PKC isozyme with isozyme-specific anchoring proteins, termed RACKs. The C2 domain of the conventional PKCs (α, βI, βII, and γ) and the C2-like domain of the novel PKCs (δ, ε, θ and η) contain at least part of the RACK-binding sites. Because the C2 domain contains also a RACK-like sequence (termed pseudo-RACK), it was proposed that this pseudo-RACK site mediates intramolecular interaction with one of the RACK-binding sites in the C2 domain itself, stabilizing the inactive conformation of PKC. To address this possibility and to study the conformational changes occuring in the C2 site following activation, we examined the presence of this interaction between the pseudo-RACK site and the RACK-binding sites in the C2 domain of βPKC. PKCs depend on calcium for their activation, and the C2 domain contains the calcium binding sites. X-ray structure of the C2 domain of βPKC shows that three Ca^{2+} ions can be coordinated by two opposing loops at one end of the domain. Starting from this X-ray structure, we have performed molecular dynamics (MD) calculations on the C2 domain of βPKC bound to three Ca^{2+} ions, two Ca^{2+} ions or in the Ca^{2+}-free state. The aim of this MD modeling was to analyze the effect of calcium on the RACK-binding sites and pseudo-RACK site, as well as on the loops that constitute the binding site for the Ca^{2+} ions. The results show that the progressive reduction of the number of Ca^{2+} ions is associated with a decrease in the number and the length of secondary structure elements, as well as with an increase in the average fluctuations over the time of simulation. These data suggest that calcium stabilizes the β-sandwich structure of the C2 domain, and thus affects two of the three RACK-binding sites within the C2 domain. We also found that the interactions between the third RACK-binding site and the pseudo-RACK site are not notably modified by the removal of Ca^{2+} ions. On that basis, we predict that the pseudo-RACK site within the C2 domain masks a RACK-binding site in another domain of PKC, possibly the V5 domain (Stebbins, E.G. & Mochly-Rosen, D. (2001) *J. Biol. Chem. 276*, 29644-29650). Finally, the MD modeling also shows that the Ca^{2+} ions are able to interact with two molecules of O-phospho-L-serine. These data suggest that Ca^{2+} ions may be directly involved in PKC binding to

---

[1] **Abbreviations**: PKC = Protein Kinase C; RACK = Receptor for Activated C Kinase; MD = Molecular Dynamics; PS = Phosphatidylserine; DG = Diacylglycerol

phosphatidylserine, an acidic lipid located exclusively on the cytoplasmic face of membranes, that is required for PKC activation.

Introduction

Protein kinase C (PKC) is a family of protein kinases that undergo translocation from one intracellular compartment to another when activated by neurotransmitters, hormones, and growth factors. Most members of this family are activated by phosphatidylserine (PS), diacylglycerol (DG), and, to different extents, by other lipid second messengers and Ca^{2+} ions (*1,2*). There are at least three subfamilies of PKCs, classified according to their homology and sensitivity to activators (*2-4*). βPKC belongs to the so-called classical PKC subfamily, or cPKC (α, βI, βII and γ kinases). The members of this class contain four conserved domains (C1, C2, C3 and C4) inter-spaced with isozyme-unique (variable or V) domains. The βI and βII PKC isozymes are splice products of the same gene and therefore differ only in their C-terminal V5 domain (*5*).

The C2 domain is found also in proteins other than PKC (*4*). Because many of these proteins bind lipids and particularly PS in a calcium-dependent manner, it was obvious to suggest that the calcium- and PS-binding sites reside within this domain (*6*). Sequence alignment studies (*4*) revealed that the C2 domains exhibit two types of topologies (type I and II), but all have a β-sandwich fold composed of 4 β-strands in each face of the structure (*7*). Based on this homology, the C2 domain was suggested to contain the calcium switch required for localization to the membrane (*8*). However, immunofluorescence studies did not agree with simple localization of the activated PKC isozymes to the plasma membrane. We found that activated PKC isozymes are each localized to unique intracellular sites and therefore suggested that this unique localization is mediated by their selective interactions with specific anchoring proteins, termed Receptors for Activated C-Kinase (RACKs, Figure 1) (*9-14*). We subsequently demonstrated that the unique cellular functions of PKC isozymes are indeed dependent on the binding of each isozyme to its corresponding RACK, bringing the active PKC within a close proximity to particular subsets of substrates and away from others (*3*).

We found that the C2 domain of cPKC mediates at least some of the direct protein-protein interactions between cPKC and RACKs (*15*). The RACK1-binding site of βPKC-C2 domain (Figure 2) was identified by sequence homology analysis with synaptotagmin, another C2 domain-containing and calcium-dependent PS-binding protein, also called p65 (*15*). We reasoned that, because the C2 domain of synaptotagmin also binds to RACK1 (albeit with a 100-fold lower

affinity) (*15*), sequences most conserved between the two domains in the βPKC-C2 domain will contain the RACK1-binding sites. Peptides corresponding to amino acids 186-198 (MDPNGLSDPYVKL, βC2-2 site; red in Figure 2), 209-216 (KQKTKTIK, βC2-1 site; orange in Figure 2) and 218-226 (SLNPEWNET, βC2-4 site; blue in Figure 2) were predicted to contain the RACK-binding sites (*16,17*).

Structures of the C2 domain obtained by X-ray diffraction and nuclear magnetic resonance (NMR) spectroscopy (*18,19*) demonstrate that these RACK-binding sequences in βPKC-C2 are located on three exposed β-strands in the domain (Figure 2B). Peptides corresponding to these three β-strands specifically inhibit activation-induced translocation of the C2-containing cPKC isozymes and their functions in cells (*16,20*). As predicted, a peptide derived from a non-conserved region of the C2 domain (βC2-3, amino acids 201-207, IPDPKSE; yellow in Figure 2), which is not adjacent to the RACK-binding strands, had no effect on PKC binding to RACK, or βPKC translocation and function in cells (*16*). It therefore appears that the C2 domain of PKC has a dual role: upon activation, the domain binds PS in a calcium-dependent manner, which results in membrane binding of the enzyme. In addition, this domain participates in specific protein-protein interactions with the corresponding RACK, bringing the activated isozyme to a close proximity with a subset of substrates and away from others, thus mediating functional specificity of this family of enzymes.

Using the same logic, we suggested that translocation activators should be agonist of PKC function, independent of the amount of second messengers that normally activate PKC (*21*). We predicted that such peptide agonists would bind the unstable transition state between inactive and activated PKC, causing exposure of the catalytic site and the RACK-binding site and thus enabling the anchoring of the enzyme to RACKs (Figure 1). Indeed, a βPKC-derived peptide, termed pseudo-RACK1 peptide or ψβRACK because of its homology to RACK1 (amino acids 241-246 (SVEIWD; green in Figure 2) within the C2 domain), binds to βPKC, activates it in the absence of PS and calcium *in vitro* and acts as a selective agonist of βPKC function *in vivo* (*22*). We proposed that ψβRACK-site in βPKC is an autoregulatory site (*17,21*). When βPKC is in an inactive conformation, the ψβRACK site interacts with the RACK1-binding site; activation of PKC exposes the RACK1-binding site, enabling the association of the enzyme with its anchoring RACK (*22*). A model for this interaction is shown in Figure 1, and the relative position of the RACK1-binding sites within C2 and the ψβRACK site are indicated in the primary structure and in the secondary structure (Figure 2A) as well as in the tertiary structure of the domain (Figure 2B).

Since βPKC binds to RACK1 upon activation with calcium and PS, we studied the conformational changes in the C2 RACK-binding sites in the absence and presence of these factors using computer

4

simulation techniques of molecular dynamics (MD). MD can provide an insight into the structure and dynamics of proteins. Although such simulations are limited by the number of conformational spaces that can be sampled, these techniques are quite effective in monitoring even subtle structural changes and variations in residue-residue interactions, also when the comparison of very similar systems is concerned (*23-27*); in particular, the effect of calcium ions on protein structure was successfully evaluated on peroxidases (*28*). Here, using MD simulations of the C2 domain of βPKC, we examined the effects of calcium binding on the RACK1-binding sites and ψβRACK-site within the C2 domain. Activated βPKC has been reported to bind two (*18*) or three (*19*) Ca^{2+} ions in the C2 domain. Therefore, MD calculations were performed on the C2 domain of βPKC with three Ca^{2+} ions (βPKC-3Ca hereafter), with two Ca^{2+} ions (βPKC-2Ca hereafter) and with no Ca^{2+} ions (βPKC hereafter), using the available X-ray structure as the starting model (15). Since a direct correlation between calcium and PS binding has been also demonstrated, a simple model was also built to examine the possibility that Ca^{2+} ions bound to the domain are directly involved in PS binding. Three molecules of O-phospho-L-serine, which mimic the headgroup of PS, were positioned near the Ca^{2+} ions in the MD structure of βPKC-3Ca. A MD simulation was also performed on this complex (βPKC-3Ca-PS hereafter). Our MD studies suggest that, although conformational changes occur within the C2 domain due to calcium and PS binding, they are unlikely to mediate the disruption of interaction of the ψβRACK-site with a RACK-binding site within the C2 domain.

Methods

All calculations were carried out using AMBER 5.0 (*29*), a program commonly used for molecular dynamics simulations of proteins (*27,30-34*). The standard AMBER 1994 force field (*35*) was used. The X-ray structure of the C2 domain of rat βPKC complexed with three Ca^{2+} ions (2.7 Å resolution, PDB entry 1A25) was used to model the starting structures (*19*). While the crystal structure contains two molecules of βPKC-C2 related by a dyad axis in the asymmetric unit (*19*), the modeling was conducted on a single molecule. This domain contains 132 residues (157-288 of the complete sequence), corresponding to 1088 heavy atoms. The water molecules found in the crystal structure were excluded, following the standard procedure for protein simulations in explicit water described in the AMBER manual (*29*). Hydrogen atoms, which are missing in the 1A25 PDB file, were added through the EDIT module of AMBER, resulting in 2173 atoms in the native structure. The Ca^{2+} ions were added to the standard AMBER residue database by the PREP module

of AMBER: they were treated as divalent cations, with a van der Waals radius of 1.60 Å, and ε (i.e. 6-12 potential well depth) of 0.1 kcal mol^{-1}, based on previous MD calculations dealing with the effect of calcium ions on the structure of peroxidases ([28]). The starting positions of the Ca^{2+} ions were set according to their coordinates in the X-ray structure, and were labeled II, III and IV, following Sutton and Sprang notation ([19]). For βPKC-2Ca, calcium II and III were chosen, on the basis of the model of Ca^{2+} binding by C2 domains depicted by Shao *et al.* in ([18]): in that work, two calcium ions were found to be bound to the C2 domain through NMR spectroscopy. No direct bond was set between the calcium ions and any protein groups, and no distance constraints were introduced to prevent a bias in the modeling, i.e. the calcium ions are free to leave the protein. A shell of TIP3P ([36]) water molecules extending 10 Å in every direction from the protein surface was created using the SOL option of the EDIT module of AMBER, resulting in the introduction of about 2100 water molecules for all the model systems. Proper counterions were generated by the CION program of AMBER and positioned near free charged surface residues of the protein in order to achieve an overall charge of zero on each system, ensuring that electrostatic interactions were not broken. A 10 Å cut-off for the evaluation of the non-bonded interactions was used, resulting in the evaluation of 2.5-2.6 10^6 pair interactions. Since proteins are systems where long-range electrostatics are expected to play an important role in determining molecular conformational energies and structures, the choice of the cut-off for non-bonded interactions is significantly important for the quality of the simulation. The value of 10 Å adopted here was shown to be ([28,32,33,37-39]) a good compromise between the requirement for accurate treatment of long-range electrostatics and the requirement for a reasonable calculation time, of which the evaluation of non-bonded interactions is by far the determinant part.

The solvent molecules were equilibrated initially by energy minimization and subsequently by performing 15 ps of MD. After energy minimization of the whole system (protein + water + counterions), MD trajectories were calculated. Temperature was initially increased from 0 to 300 K (performing three MD runs of 3 ps each at 100, 200 and 300 K respectively) and then maintained constant for the whole simulation time, coupling the protein to a thermal bath ([40]). The SHAKE algorithm ([41-43]) was applied on all bonds during all the MD runs. However, a time-step of 1.5 fs could be used only in the calculation of the trajectory for βPKC, while a time-step of 1.0 fs was used both for βPKC-3Ca and βPKC-2Ca, due to instability of the trajectory in the initial steps of the simulations. The pair list was updated every 20 steps, and coordinates and energy values were collected every 100 steps for further analysis. The simulations were performed for 1060 ps and the final 1000 ps were taken for the analysis. This time frame was chosen because βPKC system

6

reached stabilization, i.e. the structure reached an average constant RMSD[2] with respect to the starting structure, after the initial 60 ps (Figure 3). βPKC-3Ca and βPKC-2Ca equilibrated faster, in about 10 ps (Figure 3). The average structures were calculated by averaging the coordinates at the various steps of the trajectories. The average structures were then subjected to energy minimization and subsequently analyzed by the program PROCHECK (*44*) to confirm the stereochemical quality of the model structures.

In βPKC-3Ca-PS model, three molecules of O-phospho-L-serine were built by the PREP module of AMBER and initially positioned in proximity of the Ca^{2+} ions of βPKC-3Ca average structure, in order to evaluate the possibility of a direct calcium-PS interaction (*45*). Nevertheless, the initial calcium-PS distance was set larger than coordination distance, to prevent a bias in the modeling of such interaction. The internal coordinates and the parameters for O-phospho-L-serine were obtained from data for serine and PO_2 groups already present in AMBER libraries. The procedure for MD modeling of this complex was performed as described above, consisting of solvation, energy minimization, heating and dynamics. The simulation time was 600 ps, with 1.0 fs as the time-step.

Results

β**PKC-3Ca**

The MD average structure, which is shown in Figure 4A, is very similar to the original X-ray structure (*19*), with average RMSD values of 0.85 Å for the backbone and 1.46 Å for the heavy atoms. The RMSD values per residue are shown in Figure 5A. All the secondary structure elements found in the crystal structure are also present after MD, as shown in Figure 6, top scheme. The average fluctuation is 0.45±0.05 Å for the backbone and 0.52±0.21 Å for the heavy atoms. These values, which indicate the range of fluctuations of the protein over the time of simulation, are rather low, and suggest that the molecule is quite rigid. The plot in Figure 6 reports the average heavy atom fluctuation per residue; the residues with the highest relative mobility correspond to the main

---

[2] RMSD (Root Mean Square Deviation) is defined as $(\Sigma_i \Delta r_i^2/i)^{\frac{1}{2}}$, where Δr_i is the displacement of an atom in a structure with respect to a reference structure, and the sum is performed over the atoms of the backbone, or over the heavy atoms, i.e. all the atoms excluding hydrogen.

loops of the domain, i.e. loop 2-3 (residues 182-193), loop 3-4 (residues 202-209), loop 4-5 (residues 212-221) and loop 6-7 (residues 247-253). α-helix 2 (residues 280-283) also shows relatively large fluctuations.

The coordination pattern of Ca^{2+} ions in the MD structure of βPKC-3Ca is shown in Figure 7, and is in good agreement with the X-ray structure (*19*), validating our modeling procedure. That coordination is maintained during the whole βPKC-3Ca simulation. Since neither direct bonds nor distance constraints were set between Ca^{2+} ions and any protein groups, we infer that these binding sites for calcium are highly stable. The coordination sphere is completed with water molecules. Site IV, which is hexacoordinate in the crystal structure (*19*), appears heptacoordinate in the present model, with the carbonyl oxygen of Asn253 as the seventh ligand.

βPKC-3Ca-PS

Phosphatidylserine (PS) is an acidic lipid located exclusively on the cytoplasmic face of biological membranes, and is required for PKC activation (*1,2*). The exact mode of interaction of PS with the enzyme is unknown; however, it has been proposed that Ca^{2+} ions bound to the protein may be involved in PS binding by providing a positively charged site for the negatively charged headgroup of PS (*45*). To mimic PS, we have chosen a simpler molecule bearing the same headgroup as PS, i.e. O-phospho-L-serine, which was also used in the determination of the crystal structure (*19*). As described in the Methods section, in this simulation three molecules of O-phospho-L-serine (PS1, PS2 and PS3) were initially positioned close to the Ca^{2+} ions in the average structure of βPKC-3Ca. After 50 ps, the structure became stable for the remainder of 550 ps of simulation. The snapshots along this simulation (see Figure 8) show that two molecules of O-phospho-L-serine (PS1 and PS2) are able to substitute the water molecules in the coordination sphere of calcium III and IV (see Figure 7). In particular, PS1 binds calcium IV in the equatorial plane through an oxygen atom of its phosphate group and PS2 binds to both calcium III and calcium IV in an axial position, through the oxygen atoms of its carboxylate group. Conversely, the third molecule of O-phospho-L-serine (PS3), which binds calcium II for the initial 450 ps of the simulation, eventually moves away, suggesting that this interaction is not stable. Furthermore, the three PS-like molecules establish instantaneous, probably non-specific, interactions with some of the residues belonging to loop 6-7, i.e. Leu249, Thr250, Ser251 and Arg252. Though none of these interactions are stable along the entire trajectory, altogether they appreciably reduce the mobility of loop 6-7: the average value of

the fluctuations for residues 247-253 is 0.64 Å, compared with 1.00 Å for the same segment in the βPKC-3Ca system, therefore in the absence of PS. Although this simulation does not completely mimic the PKC interaction with the membrane bilayer, it further supports the previous findings that calcium may be directly involved in binding of PS (*45,46*).

βPKC-2Ca

The average MD structure of βPKC with two calcium ions is shown in Figure 4B. Removal of calcium IV from βPKC-3Ca increases the average RMSD relative to the crystal structure, with 0.98 Å of RMSD for the backbone and 1.75 Å for the heavy atoms, respectively. The values per residue are shown in Figure 5B. Comparison of Figures 4A and 4B shows that the effect of removing this Ca^{2+} ion is mainly observed on loop 6-7, which is involved in calcium coordination, and on loop 3-4, probably due to the shortening of β-strand 4 (from 209-211 to 210-211). Additional changes in secondary structures were noted: β-strand 5 and 8 are shortened (from 222-230 to 225-230 and from 271-276 to 273-276, respectively), and the first helix (amino acids 233-238) is missing after removal of calcium IV. In contrast, the second helix (α1) becomes longer (from 265-268 in βPKC-3Ca to 263-268 in βPKC-2Ca; see Figure 6, top). The average fluctuation is 0.51±0.09 Å for the backbone and 0.58±0.27 Å for the heavy atoms. Figure 6 reports the average heavy atom fluctuation per residue. That figure and analysis of Figure 4 suggest that the slight increase in the mobility of βPKC-2Ca as compared with βPKC-3Ca is due to a larger flexibility of loops 6-7 and 3-4. The removal of calcium IV results in an increased flexibility of loop 6-7, since this calcium is coordinated exclusively by residues in loop 6-7 (see Figure 7). The removal of calcium also affects loop 3-4 indirectly, because it results in a shortening of β-strand 4.

βPKC

The MD average structure of the calcium-free form is reported in Figure 4C. This figure shows that, also in the absence of Ca^{2+} ions, the global fold of the domain is maintained. However, conformations of certain regions are notably different from the calcium-bound structures.

The average RMSD of βPKC as compared to the crystal structure is higher than in the calcium-bound states; it is 1.65 Å for the backbone and 2.44 Å for the heavy atoms. The largest RMSD values are found for loops 3-4 and 6-7 (see Figure 5C), supporting the observation that these loops are the regions most affected by the progressive removal of calcium. The most striking effect of

9

calcium removal is the disappearance of the short β-strand 4 (Figures 4 and 6, top). Other secondary structure elements that differ from βPKC-2Ca (see Fig 6, top) include the interruption of β-strand 3 in the middle (residues 198-199), shortening of β-strand 7 (from 254-262 to 259-262) and lengthening of β-strand 8 to the length found in the βPKC-3Ca state (271-276). An increase of mobility for loop 3-4 is also induced, as shown in Figure 6. However, in the absence of calcium, the domain remains quite rigid: the average fluctuation is 0.57±0.08 Å for the backbone and 0.63±0.32 Å for the heavy atoms (these values are only slightly larger than the values found for βPKC-2Ca and βPKC-3Ca).

Discussion

The present MD simulations allowed the analysis of the effects of Ca^{2+} ions on the structure of the C2 domain of βPKC. We focused mainly on the regions of this domain that have a major role in previously reported biological functions (*16-18,20,22*). These regions are indicated in Figure 2 and Table 1.

The simulations were performed on the C2 domain of βPKC bound to three Ca^{2+} ions (with and without the PS-like headgroups), two Ca^{2+} ions or in the Ca^{2+}-free state. Using this analysis, we evaluated (i) the effect of Ca^{2+} on pseudo-RACK1 and RACK1-binding sites, (ii) the effect of Ca^{2+} on the regions of the domain involved in Ca^{2+} coordination, and (iii) the possible role of calcium in PS binding by the C2 domain.

Effect of calcium on pseudo-RACK1 and βC2-2 sites

As described in the Introduction, the pseudo-RACK1 sequence was predicted to be an autoregolatory site for βPKC (*21*). We suggested that, when βPKC is in an inactive conformation, pseudo-RACK1 site interacts with the RACK1-binding site within the enzyme (Figure 1). In the active form, this intramolecular interaction is interrupted, rendering the RACK1-binding site available for the interaction with the RACK ((*22*) and Figure 1). According to the structure of the C2 domain (see Figure 2B), it is evident that, among the three identified RACK1-binding sites (*16*), only the βC2-2 (red) could interact with the pseudo-RACK1 site (green). The pseudo-RACK1 site is part of strand 6, and the spatial organization of the β-sheet to which it belongs places it next and anti-parallel to residues 194-199 of strand 3. In this position, three pairs of hydrogen bonds are present between the amide proton and the carbonyl oxygen of residues Lys199-Ser241, Lys197-Glu243 and Tyr195-Trp245 (Figure 9).

10

Regardless of the presence or absence of calcium, the distances between the β-strands 194-199 and 241-246, the two central strands of a four-stranded β-sheet, remain constant in the three modeled structures. The only exception to this general behavior is the distance between Lys197 and Glu243. In βPKC-3Ca and in βPKC-2Ca this distance is constant, whereas in the absence of calcium (βPKC) this distance fluctuates. These fluctuations, which are in the range of 1-1.5 Å, could have some functional relevance, because Glu243 constitutes the crucial difference between the pseudo-RACK1 sequence in βPKC (**SVEIWD**) and the corresponding site in RACK1 (**SIKIWD**). The presence or absence of Ca^{2+} ions does not significantly affect the hydrogen bonds between the βC2-2 and the pseudo-RACK1 segments: all the H-bonds are maintained during the MD simulations on the various trajectories, thus stabilizing the interaction between these strands in the β-sandwich.

Interesting information is obtained by monitoring the behavior of the side chains (Figure 10). The fluctuations of several distances during the simulations suggest that, in the presence of three Ca^{2+} ions, there is a stable conformation in which no interaction is present between the side chains of the β-strands 3 and 6. In particular, the amine group of Lys199, which in βPKC-2Ca and in βPKC interacts with the carboxylic group of Glu243 and, weakly, with the hydroxyl group of Ser241, does not interact with these groups in βPKC-3Ca. Furthermore, an H-bond is formed between Glu243 and the amide group of Gln280, which belongs to helix 3; the distance between Glu243-Gln280 is quite constant in the presence of three Ca^{2+} ions, whereas it undergoes large fluctuations in βPKC-2Ca and in βPKC. These findings may indicate that the third Ca^{2+} ion stabilizes, at least partially, helix 3 in a position close to pseudo-RACK1, whereas two Ca^{2+} ions are not sufficient to do that. Figure 10 shows a comparison between the average structures in which the changes involving residues Lys199, Glu243 and Gln280, induced by calcium binding, are shown.

In conclusion, the interaction between pseudo-RACK1 and βC2-2 sites is a very stable strand-strand interaction in the β-sandwich, which is not markedly altered by the removal of Ca^{2+} ions. If the activation of PKC requires the dissociation of the intramolecular interaction between these two sites, it seems highly unlikely that this dissociation involves the disruption of the β-sandwich structure, and calcium binding is unlikely to result in such a dramatic conformational change. Instead, the intramolecular interaction between the pseudo-RACK1 site and a RACK-binding site may involve side chain to side chain interactions; removal of one Ca^{2+} ion induces an interaction between Glu243 (part of pseudo-RACK1) and Lys199 (immediately after βC2-2). Therefore, it is possible that calcium binding to the third site results in disruption of intramolecular interactions between the RACK-binding site and the pseudo-RACK1 site. In addition, the surface exposed to the solvent is unaltered (Table 2), suggesting that calcium binding does not change the surface

11

characteristics of this site, and the potential interaction with RACK1. Together, these data suggest that the interaction between βC2-2 and pseudo-RACK1 do not constitute a major intramolecular interaction site that is disrupted in PKC activation by calcium. Instead, we favor the possibility that the intramolecular interaction involves the pseudo-RACK1 site with a RACK-binding site outside the C2 domain. This possibility is further supported by the finding of a RACK1-binding site within the V5 region of βPKC (*47*). Examination of this possibility awaits the availability of structural information on the intact enzyme.

Effect of calcium on the other RACK1-binding sites

The βC2-1 segment, which contains a part of the RACK1-binding site (*16*) is a very basic region, on which the removal of Ca^{2+} ions has the largest effect. As noted above, the short β strand 4, which is formed by residues 209-211 in βPKC-3Ca, is shortened (210-211) in βPKC-2Ca and absent in βPKC (Figure 6, top). This loss in the secondary structure is associated to an appreciable increase in the fluctuations around this region (Figure 6). Thus, the stabilization of a certain conformation of the βC2-1 segment is clearly a calcium-induced effect, and may be related to the activation process. The presence or the absence of calcium does not affect the extent of the solvent exposed surface (Table 2), but has significant effect on its order as a consequence of reduced mobility. This increased rigidity may be presumably necessary for the recognition by the RACK.

Similar to βC2-1, the removal of Ca^{2+} ions determines a decrease in the secondary structure elements of the βC2-4 segment (Figure 6, top), although the surface exposed to the solvent is not significantly modified (Table 2). Removal of just a single Ca^{2+} ion produces the shortening of β-strand 5, where the first three residues (222-224) are in a random coil conformation both in the presence of two Ca^{2+} ions (βPKC-2Ca) and in the calcium-free form (βPKC). Nevertheless, the fluctuations in these regions are limited in all three cases (Figure 5). From these structural changes, we can infer that the βC2-4 segment requires the binding of three Ca^{2+} ions to stabilize the proper conformation for binding to RACK.

Effect of calcium on loops 2-3 and 6-7

Loops 2-3 and 6-7 are involved in calcium-binding in the C2 domain of βPKC (*19,48*). As previously predicted (*48*), the main effect of removal of Ca^{2+} ions is to increase the distance

between these loops. The removal of one Ca^{2+} ion does not significantly modify this distance, whereas in the calcium-free state (βPKC) the electrostatic repulsion among the acidic residues, deputed to bind calcium, makes loop 6-7 move away from loop 2-3. Comparison of βPKC-2Ca and βPKC structures (Figure 4B and 4C) shows that, whereas loop 2-3 does not change significantly its position, the position of loop 6-7 is notably different. This is consistent with the larger fluctuations of loop 6-7 (1-5-2.1 Å, see Figure 6) as compared with loop 2-3 (0.5-0.8 Å, see Figure 6). The motions of loop 6-7 produce the disruption of the first half of strand 7, and its shortening from 254-262 in βPKC-2Ca to 259-262 in βPKC. Furthermore, the separation of the two loops is associated with a reorganization of some hydrogen bonds in this region. Specifically, the H-bonds between the backbone H of Asp193 and a carboxylic O of Asp246 and between the backbone O of Asp193 and the backbone H of Trp247 are present only in βPKC-3Ca, whereas the H-bond between the backbone H of Asp246 and the backbone O of Asp254 is present in βPKC-3Ca as well as in βPKC-2Ca. On the other hand, only in βPKC Asp187 forms two H-bonds with Asn189 (backbone and side chain H) with one of its carboxylic oxygens. These differences between βPKC-3Ca and βPKC structures are shown in Figure 11.

On the basis of NMR studies (*18*), it was found that βPKC-C2 binds two calcium ions (corresponding to sites II and III in Figure 7), while a third ion may bind with a lower affinity. However, the crystal structure of the same domain (*19*) shows three bound calcium ions per domain. In that crystal structure, one donor atom to the third calcium ion (site IV in Figure 7) is provided by a residue from the second C2 molecule in the asymmetric unit of the crystal; in solution, this donor atom is replaced by a well-ordered, highly rigid water molecule (the axial water in Figure 7). Furthermore, Asn253 remains at a coordination distance for the entire trajectory and completes heptacoordination of calcium IV, together with another water molecule in the equatorial plane (see Figure 7). Therefore, binding site IV is already well organized to bind a calcium ion in the crystal structure, which we used as the starting conformation in βPKC-3Ca simulation, and it remains very stable as long as the coordination sphere is complete, as it happens in our simulation: the energetics of this system is such that repulsion of calcium IV does not occur, at least on MD trajectory time-scale, i.e. about 1 ns.

How is calcium involved in PS-binding?

It is well known that calcium increases the affinity of cPKC for negatively charged lipids (*49,50*). Newton and collaborators originally suggested that the positively charged surface of sheet B (β-

13

strands 3, 4, 6 and 7), determined by a cluster of lysine residues at positions 197, 199, 209, 211 and 213, may provide the binding site for PS. The decreased distance between loops 2-3 and 6-7 due to calcium binding could orient this basic face to interact with the lipids' headgroups (*51*). This hypothesis is in agreement with the X-ray structure by Sutton and Sprang (*19*) that was determined using crystals grown in the presence of O-phospho-L-serine as a headgroup analog of PS. Weak electron density was found at the surface of sheet B, such that the phosphate group was in contact with lysines 197, 199 and 211, even though the absence of strong density for the putative seryl group and specific protein contacts with it suggested that the interaction might be nonspecific (*19*). Our results show that the accessibility of this basic cluster is not reduced in the absence of calcium as compared to the calcium-bound states (see Table 2). Therefore, it does not seem likely that the calcium-induced increased affinity of PKC for negatively charged lipids is due to a larger exposure of the basic cluster on the surface of sheet B. Indeed, subsequent experimental data from Newton's group show that substitution of four lysine residues in the cluster with neutral residues does not inhibit association of βPKC with PS-enriched vesicles (*52*). Instead, our data suggest that this sequence provides part of the docking site for RACK1 (*16*), and the stabilization of the β-sandwich structure induced by calcium binding may be required for this protein-protein interaction (*52*).

As an alternative explanation, it has been also suggested that the Ca^{2+} ions bound to PKC maintain some of their coordination open to interact with the negatively charged headgroup of phospholipids (*45*). We have examined this possibility by simulating the interaction of three O-phospho-L-serine molecules with the Ca^{2+} ions in the structure of βPKC-3Ca. This MD simulation shows that only two molecules of O-phospho-L-serine are able to coordinate the three Ca^{2+} ions through the oxygen atoms of the phosphate or of the carboxylate group, by substituting the water molecules in the coordination sphere of the calcium ions (Figures 7 and 8). These data support the possibility that Ca^{2+} ions are indeed directly involved in PS binding by acting as a bridge.

The Ca^{2+} bridge model is supported by an X-ray structure of the αPKC-C2-$(Ca^{2+})_2$-PS complex by Verdaguer *et al.* (*53*), showing that one molecule of 1,2-dicaproyl-*sn*-phosphatidyl-L-serine (DCPS) is specifically coordinated to a Ca^{2+} ion and other residues in the Ca^{2+}-binding loops. In that work, a membrane-binding mechanism of the αPKC-C2 domain is suggested in which two calcium ions play different roles in membrane binding. Recent studies of the C2 domains of αPKC (*54*) and cytosolic phospholipase A_2 (*55*), both of which bind two Ca^{2+} ions, also showed that two Ca^{2+} ions play distinct roles, with one primarily involved in inducing conformational changes and the other in Ca^{2+} bridging. On this basis, we can infer similar differential roles for Ca^{2+} ions in the membrane targeting of βPKC-C2, because βPKC-3Ca-PS simulation data show that only calcium

14

III and IV are coordinated in a stable way by O-phospho-L-serine, whereas calcium II is not. On the other hand, comparison of data from βPKC-3Ca, βPKC-2Ca and βPKC simulations (see above) show that all three Ca^{2+} ions are involved in inducing conformational changes in the domain, especially in loop 6-7. Therefore, we suggest that calcium III and IV play a dual role in the membrane targeting of βPKC-C2, providing a bridge between the C2 domain and phospholipids as well as inducing conformational changes. Conversely, calcium II is not involved in bridging and its role appears limited to the stabilization of the domain structure.

In addition, in the course of βPKC-3Ca-PS simulation, O-phospho-L-serine molecules appear to interact also with protein residues of loop 6-7, reducing the mobility of that loop. This suggests that phospholipid binding may determine a further increase in the order of this region of the βPKC-C2, thus establishing a positive cooperation with Ca^{2+} binding in order to achieve a certain conformation of the domain.

This possibility is supported by a recent mutation analysis of the C2 domain of αPKC (*54*). In particular, in agreement with our findings, interactions along loop 6-7 indicate that at least two residues (Arg249 and Arg252) participate in electrostatic interaction with anionic lipids and two others (Trp245 and Trp247) participate in penetration into the membrane. Also in the above-mentioned X-ray structure of αPKC complex with DCPS (*53*), this PS-mimicking molecule is found to bind to the C2 domain of αPKC both via the calcium coordination and by direct interaction with Trp247 and Arg249. On the other hand, in the same work (*53*) the authors emphasize that phospholipid analogs, such us O-phospho-L-serine, used to analyze the binding of phospholipids to βPKC (*19*), lack the possibility of some of the interactions seen in the structure of αPKC-C2-$(Ca^{2+})_2$-PS complex. Therefore, the unstable interactions between βPKC-C2 and O-phospho-L-serine we identified in the simulation may in fact mimic the direct association of the enzyme with the lipids, and the instability could be due to the inadequacy of O-phospho-L-serine in mimicking PS. The docked model of the αPKC-C2-$(Ca^{2+})_2$-PS complex onto a model membrane proposed by Verdaguer *et al.* (*53*) suggested to us that the molecule of PS3 in βPKC-3Ca-PS simulation (see Figure 8) could be actually replaced by a longer hydrophobic tail of PS1. This model is, of course, mainly speculative.

Finally, Nalefski and collaborators compared the equilibrium and kinetic parameters of C2 domains binding to calcium and lipids (*56*). This study demonstrates that there are at least two steps in the docking of the C2 domain to membranes: a rapid calcium binding followed by a slower membrane binding. These authors further demonstrated that, although the C2 domains of various proteins share sequence homology and similar architecture, they exhibit unique coordination of calcium,

15

resulting in different kinetics of membrane docking (*56*). Our previous work on the role of RACKs in docking of activated PKC adds a third step in this process of docking, providing further mechanism to ensure specific subcellular localization of the activated enzyme and possibly increased stability for this docking.

Final considerations

The present MD simulations indicated that the progressive reduction of the number of Ca^{2+} ions bound to the C2 domain of βPKC causes a decrease in the number and the length of secondary structure elements, as well as an increase in the average fluctuations over the time of simulation. On this basis, we infer that calcium binding determines a stabilization of the β-sandwich structure of the C2 domain. In particular, we observed that this stabilization affects two regions of the C2 domain which are involved in binding of the activated form of PKC to its receptor, RACK1. These regions correspond to βC2-1 and βC2-4. This observation suggests that calcium cooperates in PKC activation by driving the RACK1-binding sites within C2 towards the most favorable conformation for the interaction with RACK1.

In addition to the effect of calcium on the structure of βC2, calcium plays an electrostatic role in PKC activation: the binding of two or three Ca^{2+} ions is expected to produce a drastic change in the electrostatic potential field around their binding sites, neutralizing the negative charge of the acidic cluster of aspartates on C2. This change in electrostatic field has been suggested to represent a molecular switch (*50,57*) that contributes to shift the enzyme to its activated form. We propose here two possible but not incompatible mechanisms for the working of this switch. In the former mechanism, Ca^{2+} ions are directly involved in PKC binding to PS: if this occurs, the same region of the C2 domain would bind both calcium and PS. This region, i.e. loops 2-3 and 6-7, would be able to interact with PS only after the reversal of its electrostatic properties induced by binding of Ca^{2+} ions. In the latter mechanism, the changes induced by calcium binding affect the domain-domain interactions between the C2 domain and other domains in PKC, which may contribute to maintaining PKC in the inactive state (*58*). As mentioned earlier, one possible domain participating in this intramolecular interaction is the V5 domain. It is located in the last 50 amino acids of PKC and constitutes the only difference between βI and βIIPKC isozymes (*3*). Our recent study showed that at least part of the RACK1-binding site in βIIPKC is located within the V5 domain of the enzyme (*47*). The βIIPKC V5 domain binds directly to RACK1 with an affinity similar to that of the isolated C2 domain enzyme (*47*). In addition, peptides derived from the βIIV5 domain inhibit

16

βIIPKC binding to RACK1 *in vitro* and inhibit βIIPKC translocation and function in cells (*47*). The presence of relatively limited interactions between the pseudo-RACK1 sequence with RACK1-binding sites within the C2 domain in our modeled structures suggests that pseudo-RACK1 site interacts with RACK-binding sites on other PKC domains. Since the V5 domain directly binds to RACK1, it may also interact with the pseudo-RACK1 sequence in the C2 domain, to mask it in the inactive state. Such V5/C2 interactions have been previously suggested (*59,60*). The first reports indicating interaction between V5 and C2 domain were provided by the work of Newton *et al.*, showing that calcium binding to the C2 domain of βPKC isozymes is affected by their V5 domains (reviewed in (*59*)). In addition, the phosphorylation of Ser660 in the V5 region increases the affinity of the enzyme to both phospholipids and calcium, presumably due to allosteric effects of the V5 domain on the C2 domain (*60*). The possibility of inducible intra-domains interactions in PKC, such as these suggested here between the C2 and V5, could be directly addressed when the complete structure of PKC becomes available.

Finally, it is still not known what are the steps that lead inactive cytosolic PKC to anchor to a particular site within the cells. There could be at least three steps, including calcium binding, lipid binding and RACK binding. The final step leads to maximal stabilization of the activated isozymes, which occurs during protein-protein binding of the PKC via the C2 domain and the V5 domain to the pre-anchored RACK1. Future studies including co-crystallographic kinetic analysis with purified components will help elucidate the question.

Acknowledgments

References

1. Parker, P.J., Kour, G., Marais, R.M., Mitchell, F., Pears, C., Schaap, D., Stabel, S., & Webster, C. (1989) *Mol. Cell. Endocrinol. 65*, 1-11

2. Nishizuka, Y. (1992) *Science 258*, 607-614

3. Mochly-Rosen, D. & Gordon, A.S. (1998) *FASEB J. 12*, 35-42

4. Nalefski, E.A. & Falke, J.J. (1996) *Protein Sci. 5*, 2375-2390

5. Coussens, L., Parker, P.J., Rhee, L., Yang-Feng, T.L., Chen, E., Waterfield, M.D., Francke, U., & Ullrich, A. (1986) *Science 233*, 859-866

6. Newton, A.C. (1996) *Curr. Biol. 6*, 806-809

7. Rizo, J. & Südhof, T.C. (1998) *J Biol Chem 273*, 15879-15882

8. Shao, X., Li, C., Fernandez, I., Zhang, X., & Rizo, J. (1997) *Neuron 18*, 133-142

9. Hyatt, S.L., Klauck, T., & Jaken, S. (1990) *Mol. Carcinogen. 3*, 45-53

10. Mochly-Rosen, D., Henrich, C.J., Cheever, L., Khaner, H., & Simpson, P.C. (1990) *Mol. Biol. Cell. 1*, 693-706

11. Disatnik, M.H., Buraggi, G., & Mochly-Rosen, D. (1994) *Exp. Cell Res. 210*, 287-297

12. Lehel, C., Olah, Z., Jakab, G., & Anderson, W.B. (1995) *Proc. Natl. Acad. Sci. U. S. A. 92*, 1406-1410

13. Gordon, A.S., Yao, L., Wu, Z.L., Coe, I.R., & Diamond, I. (1997) *Mol. Pharmacol. 52* , 554-559

14. Mochly-Rosen, D., Khaner, H., & Lopez, J. (1991) *Proc. Natl. Acad. Sci. U. S. A. 88*, 3997-4000

15. Mochly-Rosen, D., Miller, K.G., Scheller, R.H., Khaner, H., Lopez, J., & Smith, B.L. (1992) *Biochemistry 31*, 8120-8124

16. Ron, D., Luo, J., & Mochly-Rosen, D. (1995) *J. Biol. Chem. 270*, 24180-24187

17. Souroujon, M.C. & Mochly-Rosen, D. (1998) *Nat. Biotechnol. 16*, 919-924

18. Shao, X., Davletov, B.A., Sutton, R.B., & Rizo, J. (1996) *Science 273*, 248-251

19. Sutton, R.B. & Sprang, S.R. (1998) *Structure 6*, 1395-1405

20. Mochly-Rosen, D. (1995) *Science 268*, 247-251

21. Ron, D., Chen, C.-H., Caldwell, J., Jamieson, L., Orr, E., & Mochly-Rosen, D. (1994) *Proc. Natl. Acad. Sci. U. S. A. 91*, 839-843

22. Ron, D. & Mochly-Rosen, D. (1995) *Proc. Natl. Acad. Sci. U. S. A. 92*, 492-496

23. McCammon, J.A. & Harvey, S.C. (1987) in *Dynamics of proteins and nucleic acids*, Cambridge University Press, Cambridge.

24. Brooks, C.L., III, Karplus, M., & Petitt, B.M. (1988) in *Proteins: a perspective of dynamics, structure and thermodynamics*, J. Wiley and Sons, New York.

25. Kollman, P.A. & Merz, K.M.Jr. (1990) *Acc. Chem. Res. 23*, 246-252

26. Van Gunsteren, W.F. & Berendsen, H.J.C. (1990) *Angew. Chem. Int. (Ed. Engl.) 298*, 992-1023

27. Van Gunsteren, W.F. (1993) *Curr Opin Struct Biol 3*, 277-281

28. Banci, L., Carloni, P., Diaz, A., & Gori Savellini, G. (1996) *JBIC 1*, 264-272

29. Pearlman, D.A., Case, D.A., Caldwell, J.W., Ross, W.S., Cheatham, T.E., Ferguson, D.M., Seibel, G.L., Singh, U.C., Weiner, P.K., & Kollman, P.A. (1997) in *AMBER 5.0*, University of California, San Francisco.

30. Van Gunsteren, W.F. & Mark, A.E. (1998) *J. Chem. Phys. 108*, 6109-6116

31. Chong, L.T., Duan, Y., Wang, L., Massova, I., & Kollman, P.A. (1999) *Proc. Natl. Acad. Sci. U. S. A. 96*, 14330-14335

32. Wang, W., Lim, W.A., Jakalian, A., Wang, J., Wang, J., Luo, R., Bayly, C.I., & Kollman, P.A. (2001) *J Am Chem Soc 123*, 3986-3994

33. Banci, L., Carloni, P., & Orioli, P.L. (1994) *Proteins Struct. Funct. Genet. 18*, 216-230

34. Banci, L., Carloni, P., La Penna, G., & Orioli, P.L. (1992) *J. Am. Chem. Soc. 114*, 6994-7001

35. Cornell, W.D., Cieplak, P., Bayly, C.I., Gould, I.R., Merz, K.M., Ferguson, D.M., Spellmeyer, D.C., Fox, T., Caldwell, J.W., & Kollman, P.A. (1995) *J. Am. Chem. Soc. 117*, 5179-5197

36. Jorgensen, W.L., Chandrasekhar, J., Madura, J., Impey, R.W., & Klein, M.L. (1983) *J. Chem. Phys. 79*, 926-935

37. Banci, L., Carloni, P., & Gori Savellini, G. (1994) *Biochemistry 33*, 12356-12366

38. Wong, K.B. & Daggett, V. (1998) *Biochemistry 37*, 11182-11192

39. Storch, E.M. & Daggett, V. (1995) *Biochemistry 34*, 9682-9693

40. Berendsen, H.J.C., Postma, J.P.M., Van Gunsteren, W.F., DiNola, A., & Haak, J.R. (1984) *J. Chem. Phys. 81*, 3684-3690

41. Rickaert, J.P., Cicotti, G., & Berendsen, H.J.C. (1977) *J. Comput. Phys. 23*, 327-341

42. Van Gunsteren, W.F. & Berendsen, H.J.C. (1977) *Mol. Phys. 34*, 1311-1327

43. Andersen, H.C. (1983) *J. Comput. Phys. 52*, 24-34

44. Laskowski, R.A., MacArthur, M.W., Moss, D.S., & Thornton, J.M. (1993) *J. Appl. Crystallogr. 26*, 283-291

45. Perisic, O., Fong, S., Lynch, D.E., Bycroft, M., & Williams, R.L. (1998) *J. Biol. Chem. 273*, 1596-1604

46. Nalefski, E.A., Slazas, M.M., & Falke, J.J. (1997) *Biochemistry 36*, 12011-12018

47. Stebbins, E.G. & Mochly-Rosen, D. (2001) *J. Biol. Chem. 276*, 29644-29650

48. Newton, A.C. (1995) *Curr. Biol. 5*, 973-977

49. Bazzi, M.D. & Nelsestuen, G.L. (1987) *Biochemistry 26*, 115-122

50. Newton, A.C. & Keranen, L.M. (1994) *Biochemistry 33*, 6651-6658

51. Newton, A.C. (1995) *J. Biol. Chem. 270*, 28495-28498

52. Edwards, A.S. & Newton, A.C. (1997) *Biochemistry 36*, 15615-15623

53. Verdaguer, N., Corbalan-Garcia, S., Ochoa, W.F., Fita, I., & Gomez-Fernandez, J.C. (1999) *EMBO J 18*, 6329-6338

54. Medkova, M. & Cho, W. (1998) *J Biol Chem 273*, 17544-17552

55. Bittova, L., Sumandea, M., & Cho, W. (1999) *J Biol Chem 274*, 9665-9672

56. Nalefski, E.A., Wisner, M.A., Chen, J.Z., Sprang, S.R., Fukuda, M., Mikoshiba, K., & Falke, J.J. (2001) *Biochemistry 40*, 3089-3100

57. Bazzi, M.D. & Nelsestuen, G.L. (1990) *Biochemistry 29*, 7624-7630

58. Pepio, A.M. & Sossin, W.S. (1998) *Biochemistry 37*, 1256-1263

59. Keranen, L.M. & Newton, A.C. (1997) *J. Biol. Chem. 272*, 25959-25967

60. Edwards, A.S. & Newton, A.C. (1997) *J. Biol. Chem. 272*, 18382-18390

Figure captions

Figure 1. Model of PKC activation. Inactive PKC is depicted as a folded rod with the pseudo-substrate autoinhibitory sequence associated with the substrate site in the catalytic domain, as well as with the pseudo-RACK sequence associated with the RACK-binding site. In the presence of PKC activators (PS/DG/calcium), the rod unfolds and the RACK-binding and substrate-binding sites become exposed, resulting in binding of PKC to its RACK and to its substrate. The pseudo-RACK peptide is thought to bind the unstable transition state between the inactive and active forms, shifting the equilibrium between the two conformations towards the active (open) one.

Figure 2. Sequence and secondary structure (β strands, green; helices, orange) (A) and ribbon diagram (B) of βPKC-C2 from X-ray structure showing the position of βC2-2 (red), βC2-3 (yellow), βC2-1 (orange), βC2-4 (blue) and $\psi\beta$RACK (green) sites. The Ca^{2+} ions are depicted as orange (site II), red (site III) and purple (IV) spheres. The main loops of the domain are labeled.

Figure 3. RMS deviations of the backbone atoms with respect to the starting structure as a function of simulation time for βPKC-3Ca (light grey), βPKC-2Ca (dark grey) and βPKC (black).

Figure 4. Minimized average structure of βPKC-3Ca (A), βPKC-2Ca (B) and βPKC (C). β-strands are shown in cyan and helices in orange/yellow. Ca^{2+} ions are shown as orange (site II), red (site III) and purple (site IV) spheres. The main loops are labeled.

Figure 5. RMSD per residue of the MD structure of βPKC-3Ca (A), βPKC-2Ca (B) and βPKC (C) with respect to the X-ray structure. The circles and the filled squares represent the values for the backbone and the heavy atoms, respectively. The positions of βC2-2 (2), βC2-3 (3), βC2-1 (1), βC2-4 (4) and $\psi\beta$RACK sites and the secondary structure pattern are shown in each panel.

Figure 6. Average fluctuations per residue, calculated as time-averaged RMSD over the heavy atoms with respect to the average structure, for βPKC-3Ca (crosses), βPKC-2Ca (circles) and βPKC (filled squares). The positions of βC2-2 (2), βC2-3 (3), βC2-1 (1), βC2-4 (4) and $\psi\beta$RACK sites and the secondary structure patterns of the three MD structures, as well as of the crystal structure, are also shown.

Figure 7. Coordination scheme of the three Ca^{2+} ions (II, III and IV) in the βPKC-3Ca structure. Dark gray (side chain) and light gray (backbone) spheres represent individual protein oxygen ligands. White spheres represent water molecules. The dotted lines indicate bond distances (no constraint has been imposed during the simulation).

Figure 8. Snapshot from βPKC-3Ca-PS simulation showing the interaction between βPKC-C2 and three molecules of O-phospho-L-serine (PS1, PS2 and PS3): PS1 and PS2 coordinate Ca^{2+} ions at sites III and IV (dotted lines), whereas PS3 establishes fluctuating interactions with residues of loop 6-7.

Figure 9. Interaction between βC2-2 and ψβRACK sites in βPKC-C2. Residues which are involved in strand-strand interaction are labeled, and backbone H (dark gray) and O (light gray) atoms which form hydrogen bonds are evidenced as spheres.

Figure 10. Comparison of the interactions between the side chains of Lys199, Glu243 and Gln280 in the three MD structures, which shows that Glu243 is H-bonded to Lys199 in βPKC and βPKC-2Ca (gold and coral, respectively), while it is H-bonded to Gln280 in βPKC-3Ca (magenta).

Figure 11. Rearrangement of the H-bond pattern around loops 2-3 and 6-7 upon calcium binding. The MD structures of βPKC (gold) and βPKC-3Ca (magenta) are compared. The residues involved are labeled (see text). The bonds involving backbone atoms only are not shown.

Tables

Table 1. Regions of the C2 domain of βPKC which have a major role in previously reported (see References) biological functions (*16,19,22*).

REGION	EFFECT ON PKC	REFERENCE
PSEUDO-RACK1 : residues 241-246 (SVEIWD)	cPKC agonist	22
βC2-2 : residues 186-198 (MDPNGLSDPYVKL)	cPKC antagonist	16
βC2-1 : residues 209-216 (KQKTKTIK)	cPKC antagonist	16
βC2-4 : residues 218-226 (SLNPEWNET)	cPKC antagonist	16
Loop 2-3 : residues 182-193 (NLVPMDPNGLSD)	Calcium binding	19
Loop 6-7 : residues 247-253 (WDLTSRN)	Calcium binding	19

Table 2. Solvent accessible surface for the residues of βC2-2, βC2-1 and βC2-4 sites in βPKC, βPKC-2Ca and βPKC-3Ca expressed as percentage on the total surface.

	Residue	βPKC-3Ca	βPKC-2Ca	βPKC
	βC2-2			
186	MET	19.6	18.8	27.2
187	ASP	13.4	11.5	35.2
188	PRO	62.1	62.7	59.8
189	ASN	38.6	47.7	41.9
190	GLY	23.4	21.8	18.7
191	LEU	23.4	21.8	23.0
192	SER	0.2	0.2	1.9
193	ASP	11.1	5.6	24.2
194	PRO	0.0	0.0	0.0
195	TYR	4.9	6.6	15.1
196	VAL	0.0	0.0	0.6
197	LYS	14.9	16.7	22.4
198	LEU	0.0	0.0	2.2
	βC2-1			
209	LYS	29.2	37.5	53.7
210	GLN	27.1	24.1	19.9
211	LYS	30.9	34.8	51.6
212	THR	0.5	0.6	6.2
213	LYS	42.3	42.6	39.3
214	THR	22.3	21.3	18.3
215	ILE	15.3	16.9	16.3
216	LYS	57.6	47.4	49.8
	βC2-4			
218	SER	12.0	10.0	8.2
219	LEU	12.7	14.2	11.7
220	ASN	35.7	33.0	36.4
221	PRO	3.6	1.1	2.5
222	GLU	42.6	41.7	37.0
223	TRP	8.5	5.9	2.4
224	ASN	31.4	36.2	35.1
225	GLU	29.8	22.4	24.8
226	THR	32.5	30.0	29.9

Figure 1.

pseudo-
RACK

substrate
binding
site

RACK
binding site

pseudo-
substrate

Inactive PKC

Transition state

PS/DG and
calcium

RACK

substrate

Active PKC

Figure 2.

A

B

Figure 3.

Figure 4.

A

Loop 4-5

Loop 2-3

Loop 6-7

N

C

Loop 3-4

B

Loop 4-5

Loop 2-3

Loop 6-7

N

C

Loop 3-4

C

Loop 4-5

Loop 2-3

Loop 6-7

N

C

Loop 3-4
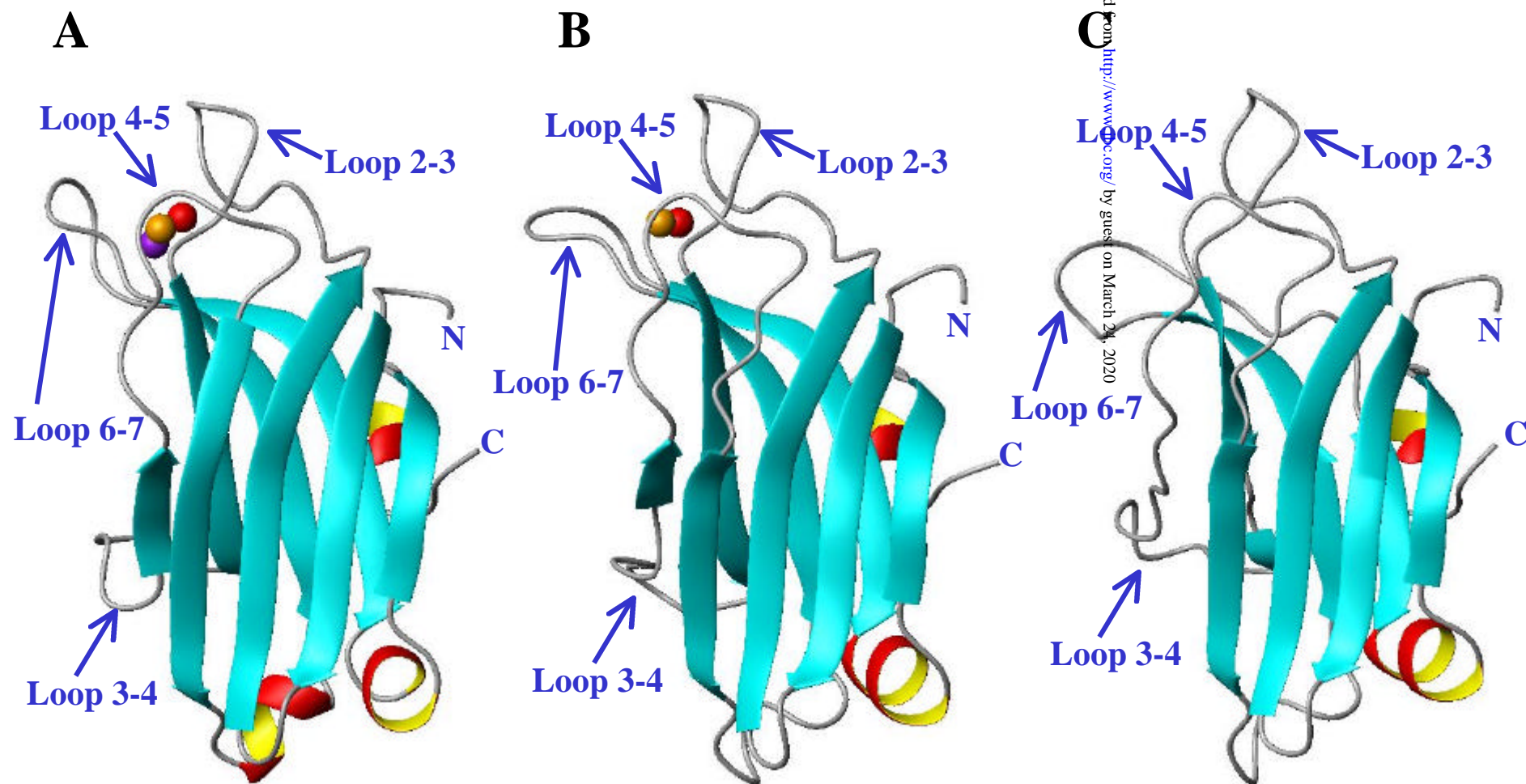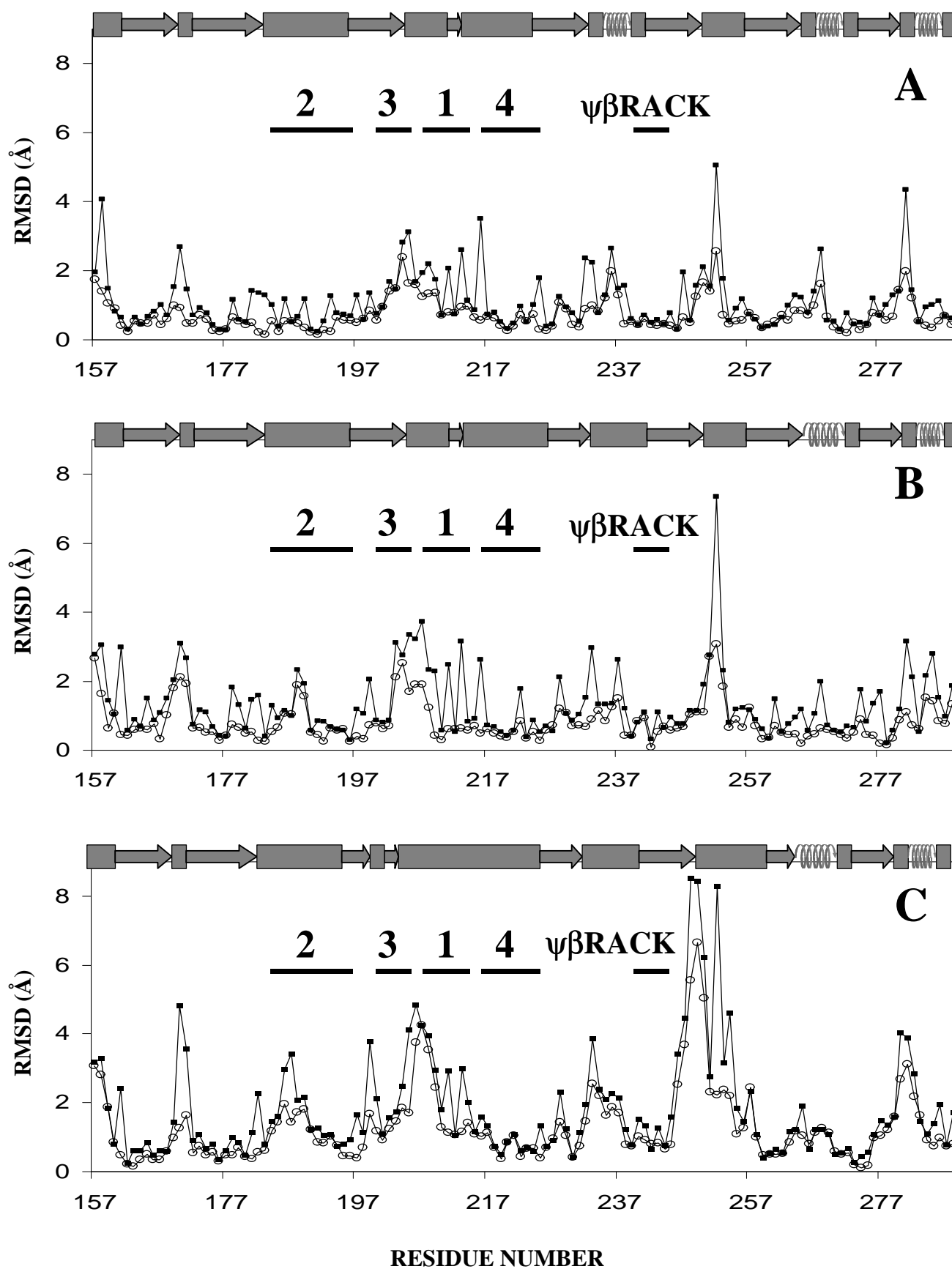
Figure 5.

Figure 6.

Figure 7.
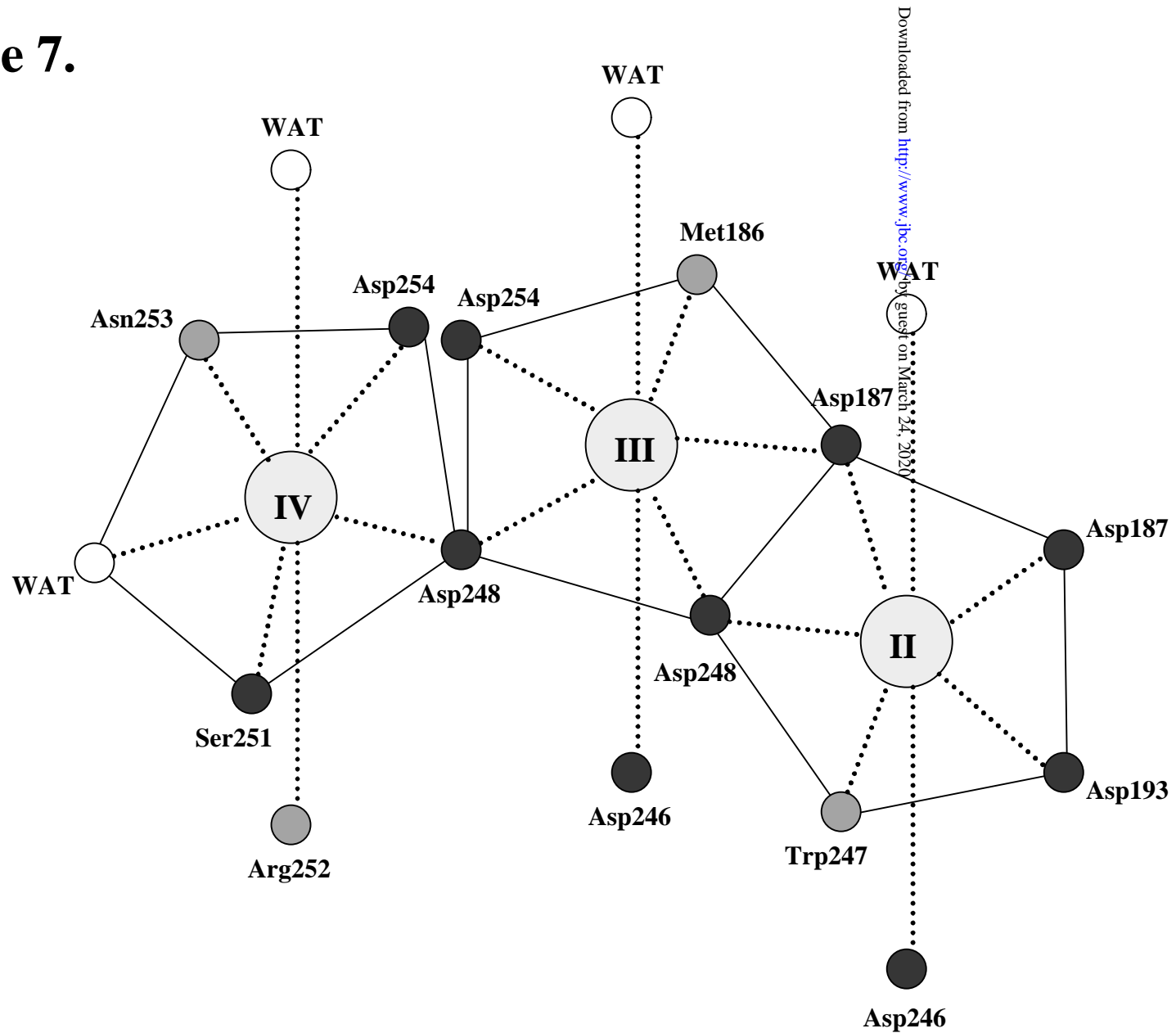
Figure 8.
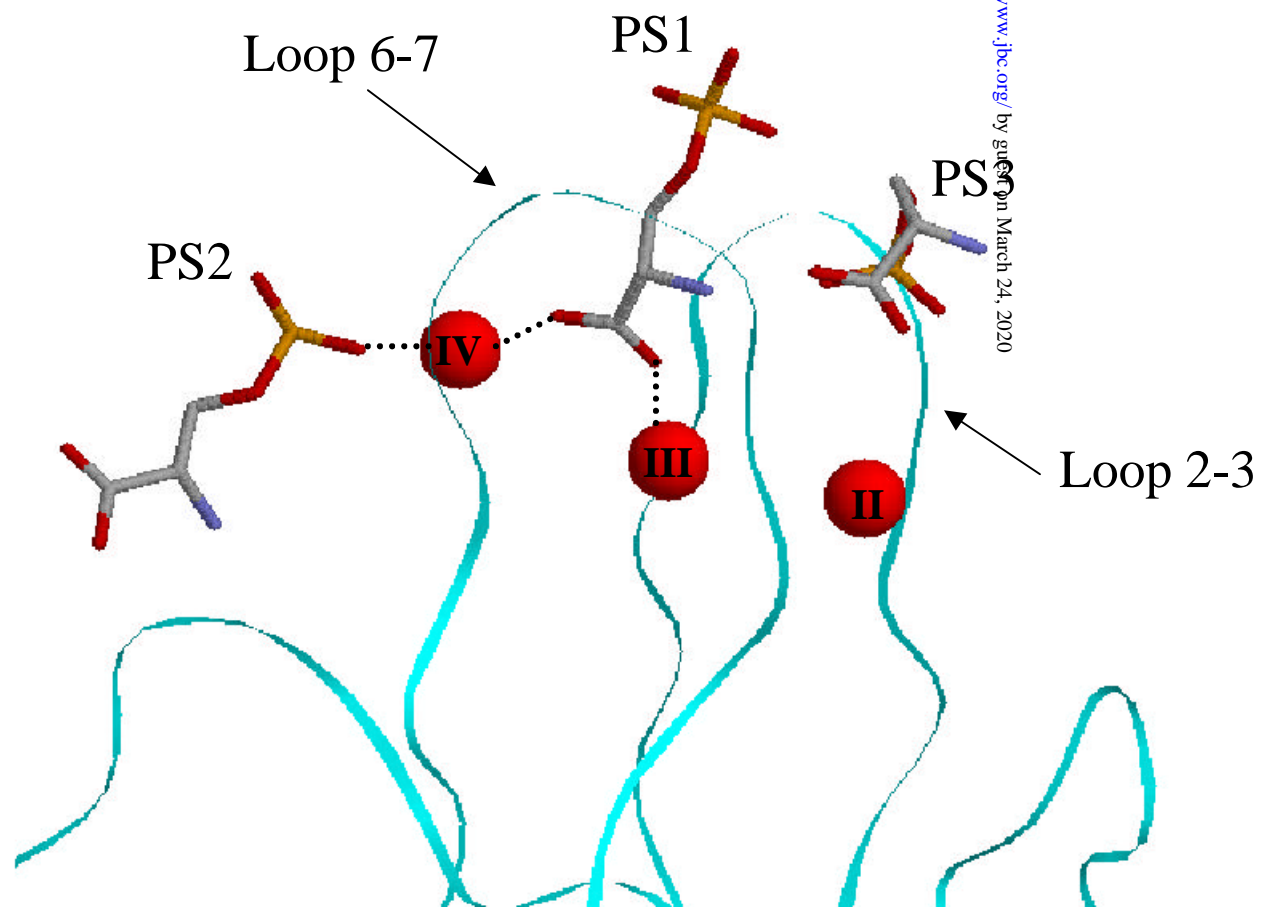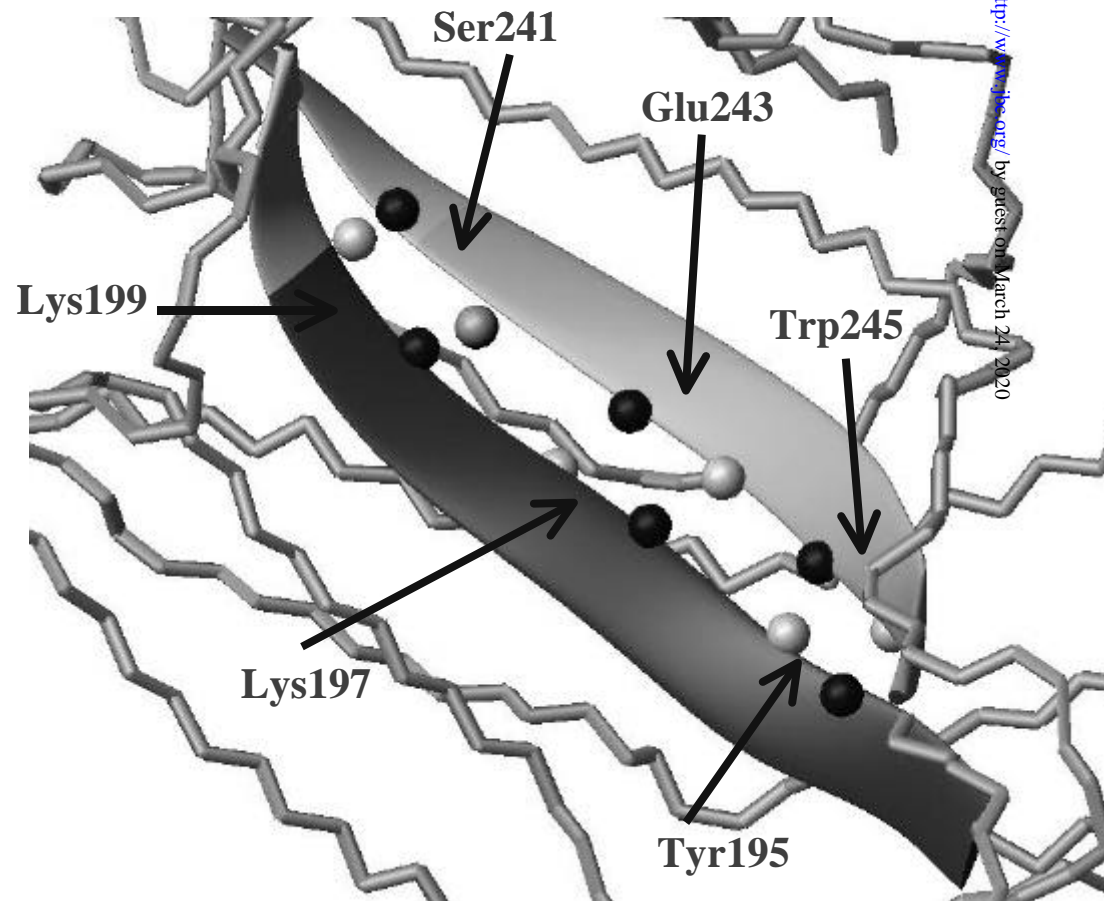
Loop 6-7

PS1

PS3

PS2

IV

III

II

Loop 2-3

Figure 9.

Figure 10.

Lys199

Gln280

Glu243

Figure 11.

Loop 6-7

Loop 2-3

Asp187

Asn189

Asp193

Asp246

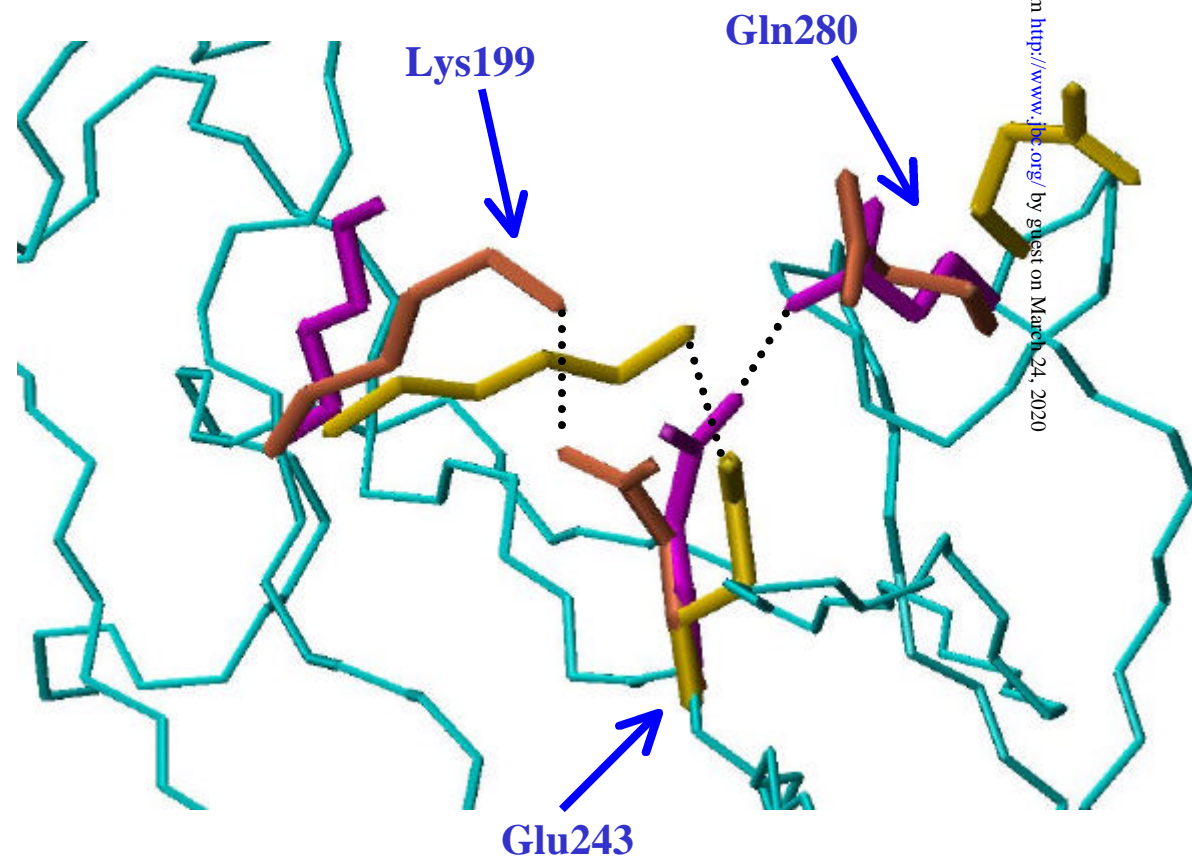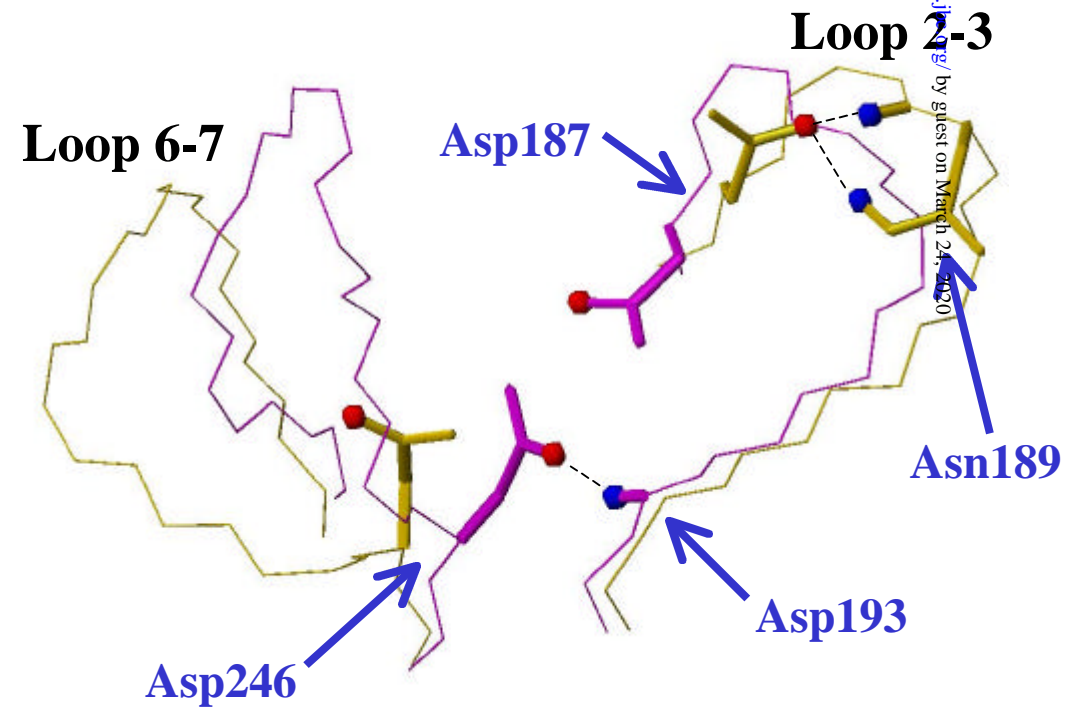**Molecular dynamics characterization of the C2 domain of protein kinase C beta**
Lucia Banci, Gabriele Cavallaro, Viktoria Kheifets and Daria Mochly-Rosen

J. Biol. Chem. published online January 8, 2002

Access the most updated version of this article at doi: 10.1074/jbc.M106875200

Alerts:
- When this article is cited
- When a correction for this article is posted

Click here to choose from all of JBC's e-mail alerts